Modelling Framework for Optimum Multiaxial 3D Woven Textile Composites

L.P. Brown[1], F. Gommer[1,2], X. Zeng[1] and A.C. Long[1]

[1]Composites Research Group, Faculty of Engineering
The University of Nottingham
Email: Louise.Brown@nottingham.ac.uk, Xuesen.Zeng@nottingham.ac.uk,
Andrew.Long@nottingham.ac.uk

[2]Department of Aeronautics
Imperial College London
Email: f.gommer@imperial.ac.uk

ABSTRACT

The application of 3D weaves has advantages over conventional uni-directional or 2D woven lay-ups. There is potential to produce near net-shaped preforms and to increase damage resistance due to the presence of through thickness reinforcement. Conventional 3D weaves typically consist of orthogonal yarns interwoven with through thickness binder yarns. This paper describes a feasibility study to find optimum architectures for 3D woven fabrics where some of the normal manufacturing constraints are relaxed. This will provide the basis for development of novel manufacturing methods based on optimum textile architectures.

A framework has been developed for the automatic generation and analysis of 3D textile geometries, utilising the open-source pre-processor TexGen. A genetic algorithm is used to select an optimum geometry by evaluating results from finite element simulations using the commercial solver Abaqus.

This paper highlights the flexibility of TexGen software to create complex 3D models by means of its Python scripting application programming interface (API). A standard layer-to-layer geometry is used as a starting point to which off-axis yarn rotations, in-plane shift of entire layers and adjustments to binder yarns can be applied. Geometric variables are selected to represent the textile architecture enabling the automation of unit cell creation and finite element analysis. A Genetic Algorithm is used to determine the optimum through thickness binder path, the number and the width of the binders, and yarn angles using a weighted objective function of the material elastic properties. The case studies show that the algorithm is efficient to converge to the optimum fibre architecture.

1 INTRODUCTION

The application of 3D weaves provides advantages over conventional uni-directional layups; there is the potential to produce near net-shaped preforms and increased damage resistance due to the presence of through thickness reinforcement. Compared to other techniques to introduce through thickness reinforcement, e.g. stitching, z-pinning, 3D weaving introduces less variability to the load carrying yarns. Despite this advantage, it has been found that 2D composites have higher damage resistance, whereas 3D composites have a higher damage tolerance [1]. The increased damage tolerance, however, is desirable as it may ensure that a damaged critical component can still perform until it can be replaced.

An overview of different modelling strategies of 3D weave materials, e.g. analytical and numerical, can be found in Ansar et al. [2]. Analytical models are usually based on classical laminate theory, CLT, and used for stiffness evaluation only. For strength predictions, numerical models are used. The models considered are usually ideal representations of yarns (fibre bundles) with perfectly aligned orientations. As this is not necessarily correct, attempts have been made to incorporate variability into the geometrical models [3]. However, the evaluation of the performance still requires a numerical solution.

Recent work [4] on optimisation of 3D woven preforms has suggested that a 50% weight saving could be achieved over standard fibre architectures for a specific application. If the fibre architecture is not constrained to orthogonal (in-plane) yarns it is possible that further weight savings can be made for structural applications. This paper describes the development of a framework for generation of 3D weave geometries which allows the relaxation of the normal manufacturing constraints, based on the work by Zeng et al. [4]. This will form the basis for the exploration of novel textile architectures which could be designed to achieve an optimum solution for a particular application.

The previous optimisation work used a Genetic Algorithm (GA) in Matlab® to derive optimum yarn bundle paths for maximum buckling resistance by evaluating numerically derived elastic properties using TexGen [5, 6] models. Internal variability of fibre bundles [7, 8] or possible variations along yarn paths [9, 10] are ignored and yarns are modelled as homogenised solids. Relaxing technical constraints applied to conventional 3D weaving leads to a potentially infinite design space. In this work, therefore, constraints were relaxed gradually, starting with rotation of yarns in either one or multiple layers. Variation of binder yarn path, in-plane shifting of entire layers and adaptation of yarn cross-sections were then also considered, but are not addressed in this paper.

2 OPTIMISATION FRAMEWORK

The framework developed integrates a unit cell finite element (FE) modelling technique within a GA. The TexGen Python scripting API is used to create textile models which can be specified by a set of parameters. Python scripts executed in the FE solver Abaqus call the TexGen functions so that model creation and the subsequent prediction of material properties can be integrated into one operation. These material properties are used to calculate an objective function value (OFV) which is used by the GA to select optimum textile geometries. The overall workflow of the framework is shown in Figure 1. The details of the GA selected and evaluation of its performance are described in [4]. This paper concentrates on the mechanism by which the data is transferred, the process which is followed in order to execute the optimisation process and the use of TexGen to create the various textile models.

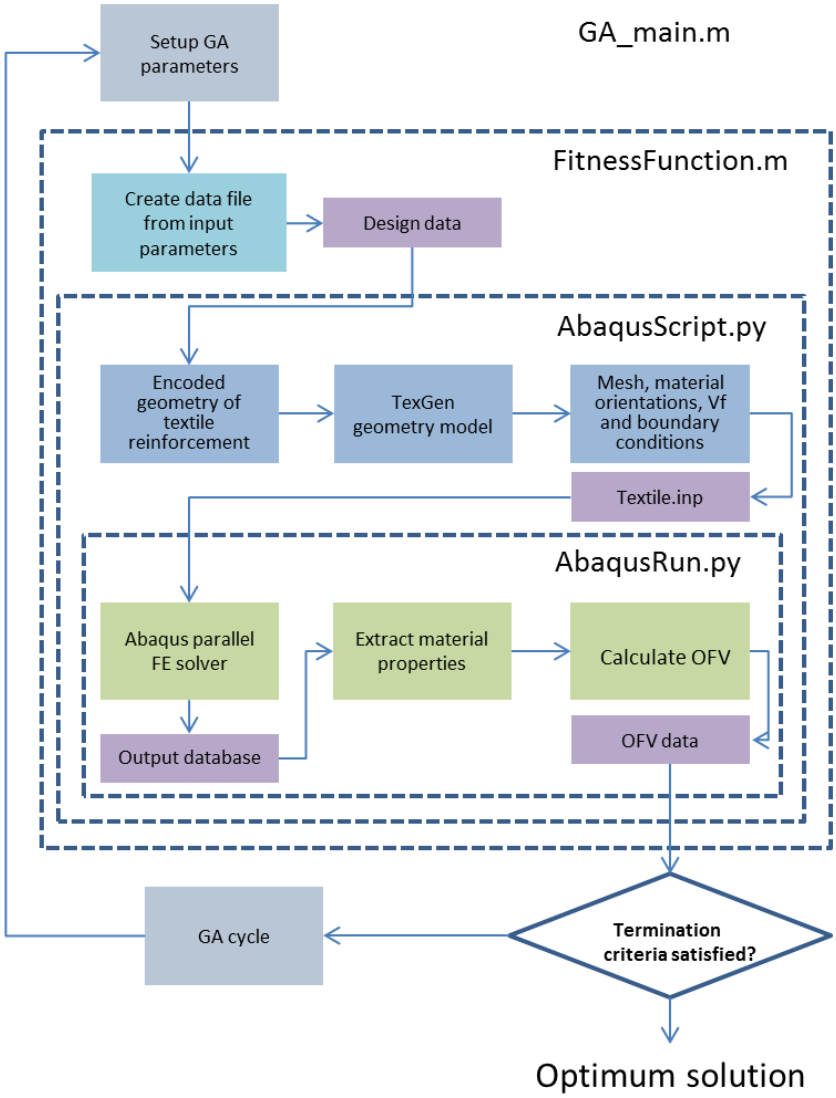

Figure 1. Workflow for the optimisation framework

The framework is run from a Matlab script which uses the standard GA algorithm built into Matlab. Initial parameters are set up, including the population size, elite number and the fitness function. The fitness function, in this case also a Matlab script, uses the parameterised data selected by the GA, converts this into a data file and subsequently starts Abaqus, specifying the Python function to be called from within Abaqus. The parameters selected by the GA and used as input for generating the textile model are a set of integers, an example of which is shown in Table 1.

The Abaqus script calls a TexGen Python script to create a geometric textile model based on the data file, as specified in Table 1, which is transferred from the GA. From this, the geometry is automatically discretised into a 3D solid voxel mesh and an Abaqus input file is created which specifies periodic boundary conditions [11] and includes the yarn orientations and fibre volume fractions calculated for the yarn elements in the mesh. From this input file, the FE simulation is run, evaluating three axial and three shear load cases. The resulting ODB file is then interrogated to extract the homogenised elastic properties of the specified textile. These properties are subsequently used to calculate the objective function value as described in Section 4.1. The GA continues to create new data sets, evaluates results as described above and stops when the

termination criteria specified in the GA setup have been satisfied, for example the objective function minima is found.

Parameter	Value
Number of binder layers	1
Binder position 1	6
Binder position 2	0
Binder position 3	6
Binder position 4	0
Index for selection of minimum rotation angle	2
Index of layer to be rotated, R1	2
Index of layer to be rotated, R2	3
Boolean for single or multiple rotation angles	0

Table 1. Example parameterised data selected by genetic algorithm for specifying textile model

3 AUTOMATIC GENERATION OF TEXTILE GEOMETRIES

This section describes elements of the textile geometry model which can be parameterized and used as input to the genetic algorithm for subsequent optimization. The structure of the 3D weave class in TexGen provides an ideal starting point.

3.1 Model Type

There are currently three types of 3D weave geometries which can be automatically generated by TexGen: orthogonal, angle interlock and layer-to-layer, all of which are created using the same CTextile3DWeave base class. The orthogonal weave is a specific type of layer-to-layer weave and the angle interlock can be achieved by parallel shift of layers in the layer-to-layer geometry. The latter was therefore chosen as the basis for the optimisation framework described in this paper.
Several parameters are set in order to define the textile [12]: number of warp & binder yarns, n_x, number of weft yarns, n_y, number of weft layers, n_{ly}, x-yarn spacing, s_x, weft yarn spacing, s_y and number of binder layers, n_{bl}. A schematic of how these are defined is shown in Figure 2a. In addition, shape parameters are set for the different yarn types: warp yarn heights, h_x, weft yarn heights, h_y, binder yarn heights, h_b, warp yarn widths, w_x, weft yarn widths, w_y and binder yarn widths, w_b.

Several constraints must be satisfied in order to retain integrity of the weave. For the case where no straight x-yarns are present and $n_x = n_{bind} = 2$, the stacks of binder yarns can be denoted as A_z and B_z. If B_z is also considered to be anti-symmetric to A_z then only the z-positions, i_z, of A_z need to be defined at intersections with the weft yarns i_x, i_y (**Error! Reference source not found.**). All i_z positions are integers which indicate layer positions, starting at index 0. The maximum position a binder can have is:

$$\max(i_z) = n_{ly} \tag{1}$$

The binder positions, i_z, can be set at all weft yarn intersections, i_x, i_y, shown in Figure 2b. However, these binder z-positions positions are bound between:

$$0 \leq A_z \leq n_{ly} \tag{2}$$

$$0 \leq B_z \leq n_{ly} \tag{3}$$

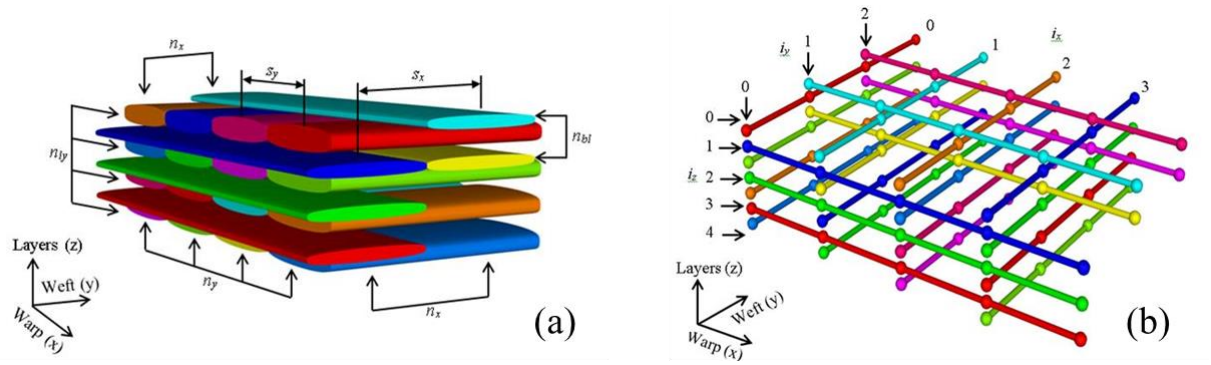

Figure 2. a) Example 3D textile geometry created with: n_{ly} = 4, n_x = 2, n_y = 4, s_x = 1, s_y = 1, h_x = 0.1, h_y = 0.2, and n_{bl} = 2 b) Example yarn paths and nodes of a 3D weave before binder positions are set: n_x = 3 (n_{warp} = 1 and n_{bind} = 2), n_y = 4, n_{bl} = 2, n_{ly}=4.

To ensure that the binder can interlace with the weft yarns and provides geometrical stability to the textile it is necessary that there are fewer binders in a stack than weft yarns present:

$$0 \leq n_{bl} \leq n_{ly} \tag{4}$$

Furthermore, it is necessary that a binder goes over the top layer and under the bottom layer of each weft stack at least once.

$$0 \in A_z \quad \text{and} \quad n_{ly} - n_{bl} \in B_z \tag{5}$$

To ensure that the textile does not separate between the binders, A_z and B_z, it needs to be ensured that the stacks of binders intersect at least once:

$$B_z \geq A_z + (n_{bl} - 1) \tag{6}$$

3.2 Introduction of off-axis yarn orientations

In this study rotation of layers is considered in order to introduce off-axis yarn orientations. This can be achieved by two means: rotation of an entire layer around a fixed point (Figure 3a) or rotation of individual yarns at fixed individual positions which are located along a straight line (Figure 3b), effectively shearing the layer.

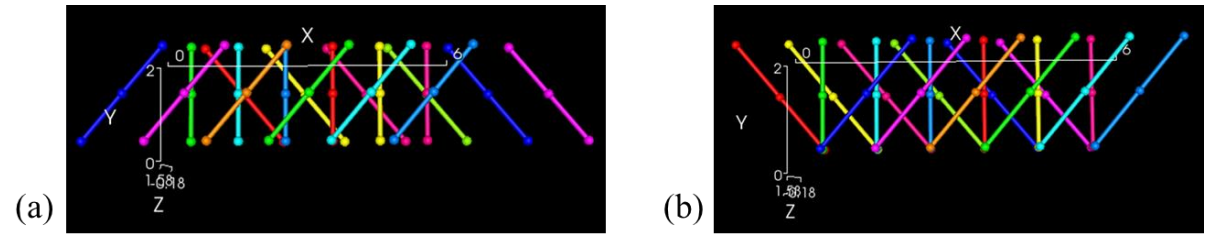

Figure 3. a) In-plane rotation of all yarns about a single fixed point. b) Rotation of individual yarns about a point at the end of each yarn.

Rotation of an entire layer has the benefit of retaining the structure of the textile layer but has the disadvantage of creating a varying pattern of gaps between the layers which can lead to complex binder paths, even when only two layers are considered (Figure 4a). In contrast shearing the layer simplifies the binder path choices (Figure 4b) but reduces the spacing between yarns which both limits the space for binder yarns to pass through and adds the limitation introduced by the locking angle of a layer as the angle increases, resulting in parallel yarns touching each other.

Shearing the yarns in a layer also has the effect of increasing the fibre volume fraction, V_f, within that layer. Both the dimensions of the yarns in the layer and/or the shape can be adjusted in

order to preserve the original V_f. In the remainder of this work, it is shear rotations which are referred to when discussing rotations.

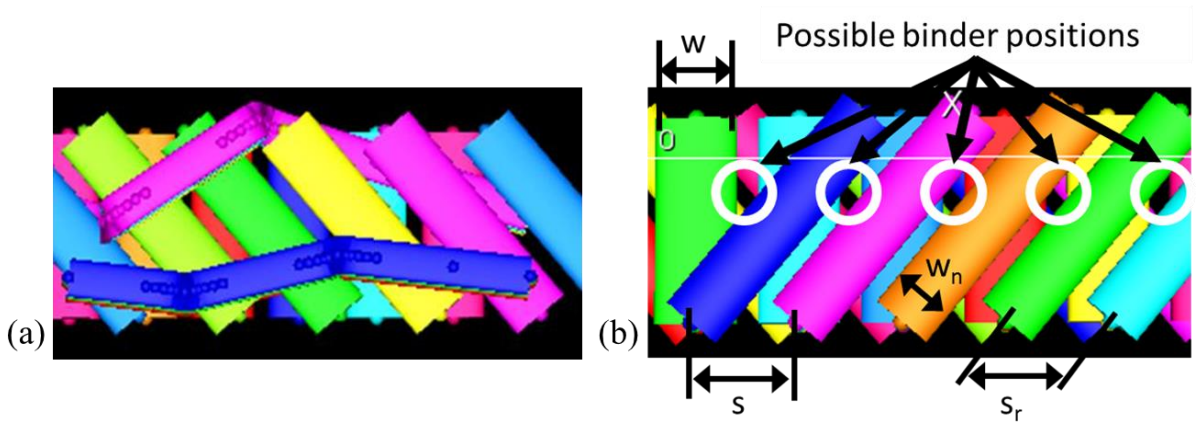

Figure 4. a) Complex binder path through two layers of yarns b) Regular spaces created by shearing of layer

3.3 Viable yarn rotation angles for creation of unit cells

Given the constraint that the textile consists of load carrying weft yarns and two anti-symmetric binder yarns, the size of a unit cell will be a function of the binder spacing when layers are rotated (Figure 5). The unit cell dimensions can be defined as a function of the rotation angle, θ:

$$uc_y = n_{bind}\frac{s}{\tan(\min|\theta|)} \quad \text{or} \quad uc_y = n_{bind} s \tan(90 - \min|\theta|) \tag{7}$$

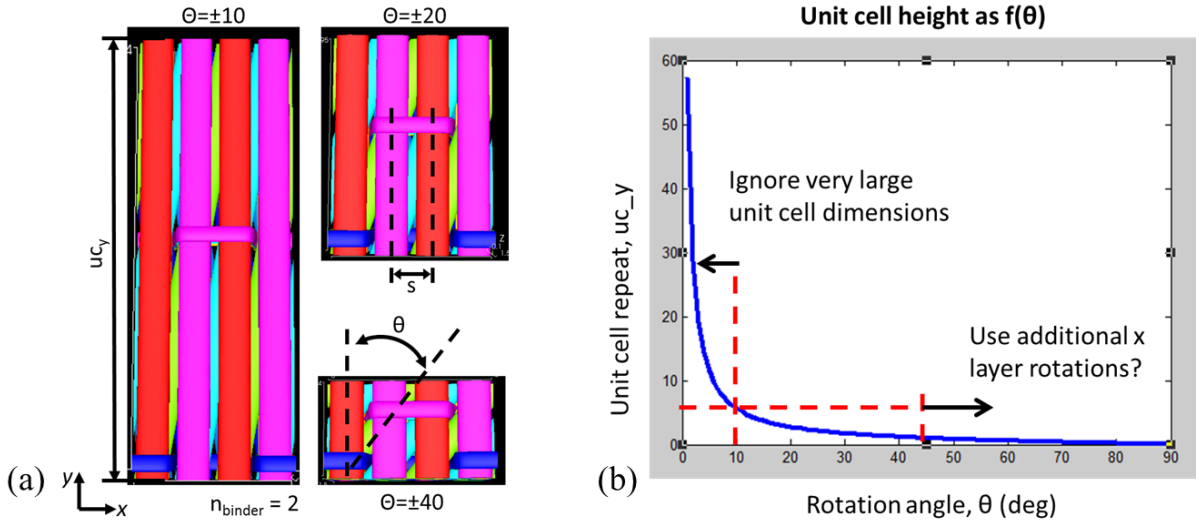

Figure 5. a) Change in unit cell dimension for different rotation angles, θ, ($n_{bind} = 2$). b) Unit cell dimension, uc_y, as a function of rotation angle, θ.

For practicality the useable range of rotation angles is limited to approximately 20° to 45-50°. Very small angles would result in very large unit cells and very large angles would reach the limit imposed by the locking angle of the yarns. The rotations also affect the binder spacing, s_b, which becomes a function of the minimum rotation angle:

$$s_b = \frac{uc_y}{n_{bind}} \tag{8}$$

With a given binder width, w_b, the maximum possible width of a straight *x*- (warp) yarn, w_x, if specified, becomes:

$$w_x = \frac{uc_y}{n_{bind}} - w_b \tag{9}$$

For small rotation angles this information may be used to maximise the amount of load carrying yarns in a layer.

3.4 Multiple rotated layers

Additional rotated layers can be included in the textile, considering the requirement to maintain symmetry of the unit cell. The rotated layers must have common intersection points with the straight yarns, thus ensuring space for the binder yarns to penetrate the entire stack (Figure 6a). As the minimum rotation angle, θ, determines the unit cell dimension by Equation (7), any possible additional rotation angle, θ_i, which ensures unit cell symmetry can be calculated by:

$$\theta_i = \tan^{-1}\left(i\frac{2s}{uc_y}\right) \text{ with } i \in \mathbb{N} = \{1,2,\dots,n_y\} \tag{10}$$

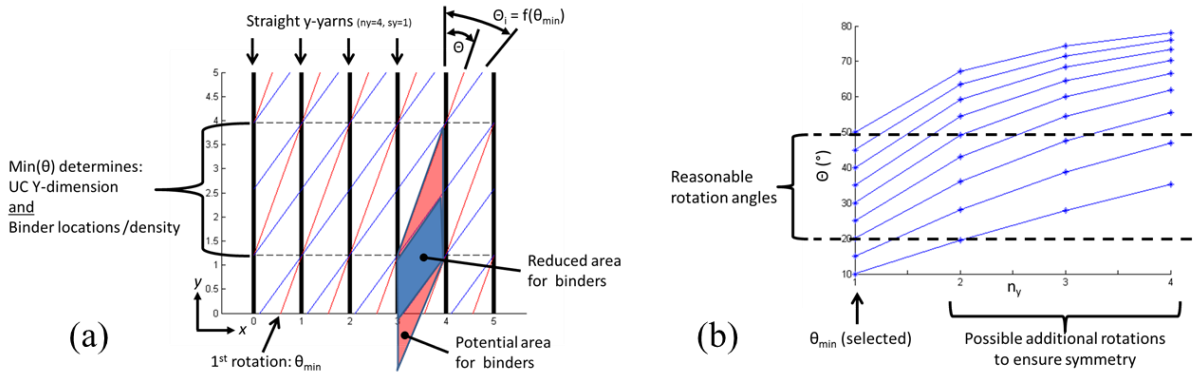

Figure 6. a) Schematic of yarn path centrelines for two different rotation angles, showing a possible area for binder yarn insertion. b) Examples of possible yarn rotation angle combinations.

Possible combinations of rotation angles based on initial selected angles are shown in Figure 6b with the horizontal dashed lines indicating the area of viable rotation angles as discussed in Section 3.3.

4 OPTIMISATION

4.1 Selection of objective function value

A number of different criteria can be used to evaluate the performance of a composite. One of these is the buckling coefficient β [13].

$$\beta = \frac{D_{11} + 2D_{66}}{\sqrt{D_{11}D_{22}}} \tag{11}$$

This coefficient describes the resistance of a composite plate against buckling and is based on a number of bending stiffness coefficients:

$$D_{11} = \frac{E_{11}}{12(1 - \nu_{12}\nu_{21})} \tag{12}$$

$$D_{22} = \frac{E_{22}}{12(1 - \nu_{12}\nu_{21})} \tag{13}$$

$$D_{12} = \frac{E_{11}\nu_{12}}{12(1 - \nu_{12}\nu_{21})} \tag{14}$$

$$D_{21} = \frac{E_{11}\nu_{21}}{12(1 - \nu_{12}\nu_{21})} \tag{15}$$

$$D_{66} = \frac{G_{12}}{12} \tag{16}$$

Other bending stiffness coefficients can be achieved using the bending, *EI*, torsion, *GJ*, or bending torsion, *K*, rigidity

$$EI = c\left(D_{22} - \frac{D_{12}^2}{D_{11}}\right) \tag{17}$$

$$GJ = 4c\left(D_{66} - \frac{D_{16}^2}{D_{11}}\right) \tag{18}$$

$$K = 2c\left(D_{26} - \frac{D_{12}D_{16}}{D_{11}}\right) \tag{19}$$

where *c* is a constant geometrical parameter.

Different criteria can be combined to give a single objective function value, OFV. In order to optimise a composite to achieve a set of target values, a function is selected which will be at a minimum for those target values, for example a parabolic function. Smaller as well as larger function values are penalised. Parameters are normalised with target values, P_{target}, to ensure comparability. The objective function will then be in the form:

$$OFV = \sum_{i=1}^{n}\left(\frac{P_i}{P_{target}} - 1\right)^2 \tag{20}$$

Another alternative is, for example, to weight different normalised components, P_i:

$$OFV = \sum_{i=1}^{n} w_i P_i \tag{21}$$

The magnitude of the individual weights, w_i, can be selected as desired. When using the optimisation framework the OFV can be specified depending on the specific application being considered.

4.2 Target value optimisation

The framework was tested for a number of optimisation runs with target values for a material provided by an industrial partner. Equation (20) was used in order to minimise the OFV for the combination of property values (Table 2). The initial minimum layer rotations allowable were in the range 20° and 50° as described in Section 3.3. For simplicity, only a maximum of 2 layer rotations and fixed yarn geometries were used for lay-ups containing 6 and 10 layers and only a single binder yarn (n_{bl} = 1). The layer rotations were limited to i = 1 or i = 2 according to Equation

(10). The warp (x) yarn width, w_x, was maximised which is a function of the rotation angle, Eq. (9). The results in Table 2 show results from optimisation runs with differing start values as well as those from a previous study with yarn angles limited to 0/90° and a set of manually selected yarn angles. Figure 7 shows the result of the optimisation run for the textile with the lowest OFV shown in Table 2.

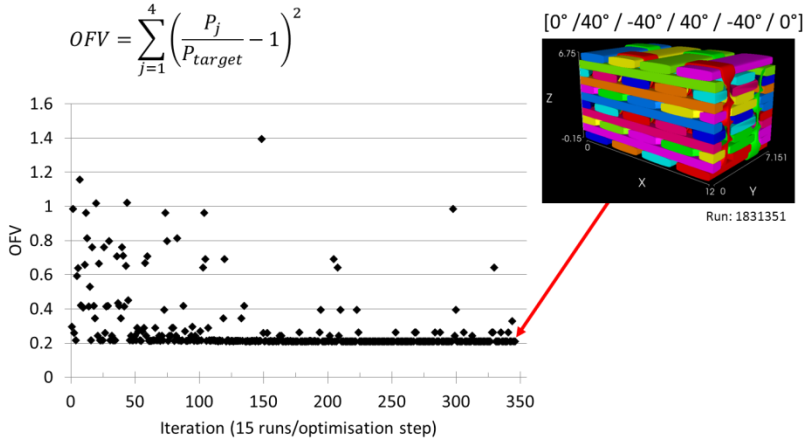

Figure 7. Genetic algorithm optimisation run and resulting unit cell

	(Selected) Lay-up	E_x (GPa)	E_y (GPa)	G_{xy} (GPa)	ν_{xy}	OFV
Target	10 layers	47	69	22	0.27	0.00
Previous study [4]	10x 90° layers (90°/0°)	52	68	4	0.04	1.41
Manual selection	$[0° / 30° / -49°]_S$	53	72	14	0.23	0.48
Optimisation Run 1	$[0° /40° / -40°]_S$	57	50	16	0.26	0.20
Optimisation Run 2	$[50 / 0° / -50° / 0° / 0°]_S$	54	57	10	0.15	0.56
Optimisation Run 3	$[0° /54° / -35°]_S$ Switched *Ex –Ey* targets	48	69	15	0.27	0.40

Table 2. Target mechanical properties provided by an industrial partner and resulting optimum configurations with corresponding OFV.

The selection of rotation angles to minimise the OFV (Table 2) are not ones which are commonly used in composite engineering at present. This highlights the potential of optimising any lay-up when using a more comprehensive design function such as the framework presented here.

5 CONCLUSIONS

A framework has been developed for optimisation of multiaxial 3D textile composites which will select optimum layer rotation angles, binder path and weft yarn width using an OFV selected for the required design properties. This will facilitate the future investigation of optimum geometries for multiaxial 3D woven textile composites, ignoring any possible current manufacturing constraints. The fully automated framework is based on utilising geometric models generated in TexGen. These models are based on the input data of an optimisation function and the analysis by a FE solver. This allows the systematic analysis of a large number of design possibilities and structure optimisation for any number of design parameters

Future work could include inclusion of additional symmetries in the periodic boundary conditions, therefore reducing computational time for the FE analyses and making the optimisation of material strength a possibility. Currently the large computational time required for strength predictions make this unrealistic. Specification of surface element sets for individual yarns in TexGen would also enable flow boundary conditions to be assigned for resin flow simulation and permeability prediction at the same time as predicting elastic mechanical properties in Abaqus.

6 ACKNOWLEDGEMENTS

This work was supported by the Engineering and Physical Sciences Research Council [grant number: EP/IO33513/1], through the EPSRC Centre for Innovative Manufacturing in Composites (CIMComp) as a 6 month feasibility study.

REFERENCES

1. Walter, T., *Characterization of delamination in 3D woven composites under static and dynamic loading*. 2011, University of Florida.
2. Ansar, M., W. Xinwei, and Z. Chouwei, *Modeling strategies of 3D woven composites: A review*. Composite Structures, 2011. **93**(8): p. 1947-1963.
3. El Said, B., S. Green, and S.R. Hallett, *Kinematic modelling of 3D woven fabric deformation for structural scale features.* Composites Part A: Applied Science and Manufacturing, 2014. **57**(0): p. 95-107.
4. Zeng, X., A.C. Long, I. Ashcroft, and P. Potluri, *Fibre architecture design of 3D woven composite with genetic algorithms - a unit cell based optimisation framework and performance assessment*, in *20th International Conference on Composite Materials (ICCM20)*. 2015: Copenhagen, Denmark.
5. Long, A.C. and L.P. Brown, *Modelling the geometry of textile reinforcements for composites: TexGen*, in *Composite reinforcements for optimum performance*, P. Boisse, Editor. 2011, Woodhead Publishing Ltd.: Cambridge. p. 239–264.
6. The_University_of_Nottingham. *TexGen*. 2014 Sep. 2015]; Available from: http://texgen.sourceforge.net/.
7. Gommer, F., K.C.A. Wedgwood, and L.P. Brown, *Stochastic reconstruction of filament paths in fibre bundles based on two-dimensional input data.* Composites Part A: Applied Science and Manufacturing, 2015. **76**(0): p. 262-271.
8. Czabaj, M.W., M.L. Riccio, and W.W. Whitacre, *Numerical reconstruction of graphite/epoxy composite microstructure based on sub-micron resolution X-ray computed tomography*. Composites Science and Technology, 2014. **105**: p. 174-182.
9. Dai, S., P.R. Cunningham, S. Marshall, and C. Silva, *Influence of fibre architecture on the tensile, compressive and flexural behaviour of 3D woven composites.* Composites Part A: Applied Science and Manufacturing, 2015. **69**: p. 195-207.
10. Gommer, F., L P Brown, and R. Brooks, *Quantification of mesoscale variability and geometrical reconstruction of a textile.* Journal of Composite Materials, 2015. **0**(0): p. 1-12.
11. Li, S. and A. Wongsto, *Unit cells for micromechanical analyses of particle-reinforced composites.* Mechanics of Materials, 2004. **36**(7): p. 543-572.
12. Brown, L.P., F. Gommer, A.C. Long, M.Y. Matveev, X. Zeng, and S. Yan, *TexGen scripting guide*. 2015, University of Nottingham.
13. Weaver, P. and M. Nemeth, *Bounds on Flexural Properties and Buckling Response for Symmetrically Laminated Composite Plates.* Journal of Engineering Mechanics, 2007. **133**(11): p. 1178–1191.